Gene Therapy Fully Restores Vision to the All-Cone *Nrl*$^{-/-}$*Gucy2e*$^{-/-}$ Mouse Model of Leber Congenital Amaurosis-1

Sanford L. Boye,[1] James J. Peterson,[1] Shreyasi Choudhury,[1] Seok Hong Min,[1] Qing Ruan,[1] K. Tyler McCullough,[1] Zhonghong Zhang,[1] Elena V. Olshevskaya,[2] Igor V. Peshenko,[2] William W. Hauswirth,[1] Xi-Qin Ding,[3] Alexander M. Dizhoor,[2] and Shannon E. Boye[1,*]

[1]*Department of Ophthalmology, College of Medicine, University of Florida, Gainesville, Florida.* [2]*Department of Basic Sciences Research, Salus University, Elkins Park, Pennsylvania.* [3]*Department of Cell Biology, College of Medicine, University of Oklahoma, Oklahoma City, Oklahoma.*

Mutations in *GUCY2D* are the cause of Leber congenital amaurosis type 1 (LCA1). *GUCY2D* encodes retinal guanylate cyclase-1 (retGC1), a protein expressed exclusively in outer segments of photoreceptors and essential for timely recovery from photoexcitation. Recent clinical data show that, despite a high degree of visual disturbance stemming from a loss of cone function, LCA1 patients retain normal photoreceptor architecture, except for foveal cone outer segment abnormalities and, in some patients, foveal cone loss. These results point to the cone-rich central retina as a target for *GUCY2D* replacement. LCA1 gene replacement studies thus far have been conducted in rod-dominant models (mouse) or with vectors and organisms lacking clinical translatability. Here we investigate gene replacement in the *Nrl*$^{-/-}$*Gucy2e*$^{-/-}$ mouse, an all-cone model deficient in retGC1. We show that AAV-retGC1 treatment fully restores cone function, cone-mediated visual behavior, and guanylate cyclase activity, and preserves cones in treated *Nrl*$^{-/-}$*Gucy2e*$^{-/-}$ mice over the long-term. A novel finding was that retinal function could be restored to levels above that in *Nrl*$^{-/-}$ controls, contrasting results in other models of retGC1 deficiency. We attribute this to increased cyclase activity in treated *Nrl*$^{-/-}$*Gucy2e*$^{-/-}$ mice relative to *Nrl*$^{-/-}$ controls. Thus, *Nrl*$^{-/-}$*Gucy2e*$^{-/-}$ mice possess an expanded dynamic range in ERG response to gene replacement relative to other models. Lastly, we show that a candidate clinical vector, AAV5-GRK1-*GUCY2D*, when delivered to adult *Nrl*$^{-/-}$*Gucy2e*$^{-/-}$ mice, restores retinal function that persists for at least 6 months. Our results provide strong support for clinical application of a gene therapy targeted to the cone-rich, central retina of LCA1 patients.

INTRODUCTION

Retinal guanylate cyclases (retGCs) are enzymes expressed in the outer segments of photoreceptors that play a pivotal role in photoreceptor recovery from photoexcitation. In response to light stimulation, cGMP-gated channels close, leading to a reduction in intracellular Ca^{2+}. This lowering of Ca^{2+} serves as a signal for Ca^{2+} sensing, guanylate cyclase activating proteins (GCAPs) to active retGCs that produce cGMP, reopen cGMP-gated channels, and return the photoreceptor to its partially depolarized state.[1,2] Humans possess two retGC isoforms (retGC1 and retGC2) and three GCAPs (GCAP1, GCAP2, and GCAP3).[3–11] Multiple studies evaluating expression of retGCs in human retina confirm that, while retGC1 is expressed in the outer segments of both rods and cones, it is expressed at relatively higher levels in cones.[3,5,12,13] It was recently reported that retGC1 is the preferred target of GCAP1 *in vivo*.[14] It is not surprising, therefore, that diseases primarily affecting cone photoreceptors have been linked to defects in both retGC1 and GCAP1. Recessive Leber congenital amaurosis type 1 (LCA1) and dominant and recessive forms of cone–rod dystrophy, CORD6 and CORD, respectively, are associated with mutations

*Correspondence: Dr. Shannon E. Boye, Department of Ophthalmology, College of Medicine, University of Florida, 1600 SW Archer Road, Gainesville, FL 32610. E-mail: shannon.boye@eye.ufl.edu

DOI: 10.1089/hum.2015.053

in the gene encoding retGC1 (*GUCY2D*).[15–18] Mutations in the gene encoding GCAP1 (*GUCA1A*) are associated with dominant forms of cone and cone–rod dystrophy.[19–26]

AAV-mediated gene replacement has proven safe and efficacious for the treatment of retinal disease.[27] To date, clinical trials targeting retinal pigment epithelium to address *RPE65* Leber congenital amaurosis (LCA2) and choroideremia (CHM), retinal ganglion cells to address Leber hereditary optic neuropathy (LHON), or broad ocular cell types to address wet age-related macular degeneration have been performed.[28–31] It remains to be seen whether photoreceptor-mediated diseases such as LCA1 will be amenable to treatment. We have evaluated the effects of gene replacement on photoreceptor structure/function and higher order visual processing in two mammalian models of LCA1, each with unique disease presentation, the retGC1 knockout (GC1KO) and the retGC1/GC2 double knockout (GCDKO) mouse.[32–34] GC1KO mice carry a null mutation in *Gucy2e*, the homolog of human *GUCY2D*, and exhibit loss of cone function and progressive cone degeneration with maintenance of rod structure and variable levels of rod function. GCDKO mice carry null mutations in both *Gucy2e* and *Gucy2f* and exhibit loss of both cone and rod function and progressive loss of photoreceptor structure.[35,36] Use of the GCDKO mouse in earlier studies was motivated by several factors. First, clinicopathologic observations reported at that time suggested that LCA1 was associated with degeneration of both cones and rods.[37,38] In addition, because it lacked confounding retGC2 activity, this was the only model in which the effects of retGC1 replacement in rods and the functional efficiency of the AAV-delivered enzyme could be precisely determined. In anticipation of possible clinical trials, a thorough clinical characterization of LCA1 was recently performed.[39] Interestingly, this revealed that the primary functional deficit in patients resides in cone photoreceptors. The majority of patients had no cone-mediated visual function, a life-long lack of color perception and a severe loss of visual acuity. In spite of this, patients retained normal retinal laminar architecture exhibiting only abnormalities in cone outer segments and, in a few patients, foveal cone losses. Patients also exhibited preservation of rod structure and variable levels of rod function. Notably, the finding in many patients that central cones are maintained despite their profound dysfunction points squarely to the fovea as the logical treatment target.

The unique retinal anatomy of primates, that is, the presence of a central, cone-rich "fovea," presents a challenge for evaluating cone-targeted therapy in animal models. The obvious drawback of mouse models is their rod-dominant retina that lacks a cone-rich central retina.[40] The GUCY1*B chicken model of LCA1 is cone-dominant, but has several shortcomings, including the considerable phylogenetic distance from placental mammals, its rapid rate of cone loss (necessitates embryonic intervention), and the inability to evaluate cone health using antibodies predominantly designed for use in rodents.[41] The $Nrl^{-/-}$ mouse exhibits a structural and functional switching of rods to an S-cone-like phenotype, verified by ultrastructural, immunohistochemical, molecular, and electrophysiological analyses.[42–44] Utilizing the $Nrl^{-/-}$ mouse as a genetic background on which to examine other mutations/alleles associated with cone dysfunction has been useful for understanding the mechanisms of cone degeneration in various forms of achromatopsia and LCA, as well as modeling retinal dystrophies with unique foveal presentation, for example, *CEP290*-LCA.[45–47] We recently crossed the GC1KO mouse onto an $Nrl^{-/-}$ background, thereby creating an all-cone model of retGC1 deficiency. The purpose of our study was to determine the impact of AAV-mediated retGC1 expression on cone structure and function and cone-mediated visual behavior in the $Nrl^{-/-}Gucy2e^{-/-}$ mouse, a model with a retina containing a high density of exclusively cone photoreceptors. We also sought to determine if a clinically relevant vector (i.e., an AAV serotype and cellular promoter with proven efficacy in primate photoreceptors driving human *GUCY2D*) would prove therapeutic in this model at a treatment age consistent with early stage clinical application (i.e., adult mouse). We rationalized that results obtained in this study would be informative in terms of the implementation of AAV-mediated gene therapy in planned clinical trials to treat LCA1 patients.

MATERIALS AND METHODS

Mice

The $Nrl^{-/-}$ mouse line on a C57BL/6 background was provided by Dr. Anand Swaroop (National Eye Institute, Bethesda, MD) and the $GC1^{-/-}$ mouse line was provided by Dr. Wolfgang Baehr (University of Utah). Cross mating was performed to generate $Nrl^{-/-}Gucy2e^{-/-}$ mice at the University of Oklahoma Health Science Center. Founder pairs of mice were transferred to the University of Florida, where they were bred and maintained in the University of Florida Health Science Center Animal Care

Services Facility under a 12 hr/12 hr light/dark cycle. Food and water were available ad libitum. All experiments were approved by the University of Florida's Institutional Animal Care and Use Committee and conducted in accordance with the ARVO Statement for the Use of Animals in Ophthalmic and Vision Research and NIH regulations.

Adeno-associated virus vectors

Vector plasmids containing the photoreceptor-specific human rhodopsin kinase, −112 to +180 (numbers represent nucleotide positions relative to transcriptional start site), promoter (hGRK1)[48] driving either murine *Gucy2e* or human *GUCY2D* cDNA were generated and packaged into AAV8-based vector containing a single tyrosine-phenylalanine mutation at residue 733 (Y733F) or AAV5, respectively. AAV vectors were purified and titered according to previously described methods.[49,50] Resulting titers for AAV8(Y733F)-hGRK1-*Gucy2e* and AAV5-hGRK1-*GUCY2D* were 1.4×10^{13} and 2.5×10^{13} vector genomes/milliliter (vg/ml), respectively.

Subretinal injections

One microliter of AAV8(Y733F)-hGRK1-*Gucy2e* was delivered subretinally to one eye of either $Nrl^{-/-}Gucy2e^{-/-}$ or $Nrl^{-/-}$ mice. Contralateral eyes remained uninjected. Injections were performed in multiple cohorts of $Nrl^{-/-}Gucy2e^{-/-}$ mice that varied in their treatment age. Cohort 1 ($n=16$) was injected between postnatal day 35 and 47 (P35–P47). These mice were evaluated alongside age-matched $Nrl^{-/-}$ controls ($n=8$) over the long-term with electroretinography (ERG), visually guided behavior tests, optical coherence tomography (OCT), immunohistochemistry (IHC), and immunoblot. Cohort 2 ($n=7$) was injected at P18 and used alongside age-matched $Nrl^{-/-}$ controls ($n=9$) for ERG analysis and Western blot at 1 month postinjection. Cohort 3 was injected at P35 ($n=6$) and used alongside age-matched $Nrl^{-/-}$ controls ($n=3$) for guanylate cyclase activity assays at 3 months postinjection. Cohort 4 ($n=7$) was injected at P40 with 1 μl of AAV5-hGRK1-*GUCY2D* and analyzed with ERG at 1 month and 5 months postinjection. Lastly, one cohort of $Nrl^{-/-}$ mice ($n=10$) was injected with AAV8(733)-hGRK1-*Gucy2e* at P35 and analyzed by ERG analysis and IHC 1 month postinjection. A summary of all cohorts is contained within Table 1. Subretinal injections were performed as previously described.[51] Further analysis was carried out only on animals that received comparable, successful injections (>60% retinal detachment and minimal complications). It is well established that the area of vector transduction corresponds to at least the area of retinal detachment.[30,51,52]

Table 1. *A summary of cohorts evaluated*

Strain	n	*Age of injection*	*Vector*	*Outcome measures*	*Time points evaluated*
$Nrl^{-/-}Gucy2e^{-/-}$	16	P35–P47	AAV8(Y733F)-hGRK1-*Gucy2e*	ERG	1, 2, 3, and 5 months PI
$Nrl^{-/-}$	8	na	na	OKN	3 and 6 months PI
				OCT	6 months PI
				IHC	6 months PI
				WB	6 months PI
$Nrl^{-/-}Gucy2e^{-/-}$	7	P18	AAV8(Y733F)-hGRK1-*Gucy2e*	ERG	1 month PI
$Nrl^{-/-}$	7	na		WB	1 month PI
$Nrl^{-/-}Gucy2e^{-/-}$	6	P35	AAV8(Y733F)-hGRK1-*Gucy2e*	GC activity assay	3 months PI
$Nrl^{-/-}$	3	na			
$Nrl^{-/-}Gucy2e^{-/-}$	7	P40	AAV5-hGRK1-*GUCY2D*	ERG	1 and 5 months PI
$Nrl^{-/-}$	10	P35	AAV8(733)-hGRK1-*Gucy2e*	ERG	1 month PI
				IHC	1 month PI

ERG, electroretinogram; IHC, immunohistochemistry; na, not applicable; OCT, optical coherence tomography; OKN, optokinetic reflex testing; P, postnatal; PI, postinjection; WB, Western blot.

Electroretinogram

Light-adapted ERGs of $Nrl^{-/-}Gucy2e^{-/-}$ mice treated with AAV8(Y733)-hGRK1-*Gucy2e* at P35–P47 and age-matched $Nrl^{-/-}$ control mice were recorded using a UTAS Visual Diagnostic System equipped with a Big Shot Ganzfeld (LKC Technologies, Gaithersburg, MD). Mice were measured at 1 month and 2, 3, and 5 months postinjection. ERGs of $Nrl^{-/-}Gucy2e^{-/-}$ mice treated with AAV5-hGRK1-*GUCY2D* were performed at 1 month and 5 months postinjection. ERGs of $Nrl^{-/-}Gucy2e^{-/-}$ mice treated at P18 with AAV8(Y733)-hGRK1-*Gucy2e* were performed at 1 month postinjection. ERGs of $Nrl^{-/-}$ mice treated with AAV8(733)-hGRK1-*Gucy2e* were performed at 1 month postinjection. Full-spectrum responses were generated in all cohorts at all time points. M- and S-cone-derived responses were collected during the final ERG recordings (5 months postinjection). Following overnight dark adaptation, mice were exposed to a 30 cds/m^2 white background for 2 min. Photopic cone responses were elicited with four increasing light intensities (1.25, 5, 10, and 25 cds/m^2). Fifty responses with interstimulus intervals of

0.4 sec were recorded in the presence of a 20 cds/m^2 white background and averaged at each intensity. For M- and S-cone-derived signals, we used similar methods to those previously published.[53] First, mice were exposed to a rod-desensitizing 30 cds/m^2 white background for 10 min. With a background light on, M- and S-cone responses were evoked with a UV light-emitting diode (LED) of 520 and 360 nm, respectively. M cones were elicited at 0.025, 0.25, 2.5, and 25 cds/m^2 and S-cone responses were elicited at 0.0025, 0.025, 0.25, and 2.5 cds/m^2. Twenty-five flashes were applied and averaged at each intensity with interstimulus intervals of 0.43 for both M- and S-cone recordings. Amplitudes of full-spectrum, M- and S-cone-driven responses were compared with Student's *t*-test. Significance was defined as a p-value <0.05.

Behavioral analysis

Cone-mediated behavior was evaluated in AAV8(Y733)-hGRK1-*Gucy2e*-treated *Nrl*$^{-/-}$*Gucy2e*$^{-/-}$ and *Nrl*$^{-/-}$ control mice at 3 and 6 months of age using the optokinetic reflex test (optomotry, cerebral mechanics). Light-adapted spatial frequency measurements were collected as previously described.[54] Spatial frequency thresholds were compared with Student's *t*-test. Significance was defined as a p-value <0.05.

Guanylate cyclase activity assays

A separate cohort of *Nrl*$^{-/-}$*Gucy2e*$^{-/-}$ mice treated with AAV8(Y733)-hGRK1-*Gucy2e* at P35 was verified for functional rescue by ERG and then used alongside age-matched *Nrl*$^{-/-}$ control mice for guanylate cyclase activity assays as previously described.[34,55,56]

Optical coherence tomography

Spectral domain OCT was performed on *Nrl*$^{-/-}$*Gucy2e*$^{-/-}$ mice treated with AAV8(Y733)-hGRK1-*Gucy2e* at P35–P47 and age-matched *Nrl*$^{-/-}$ control mice at 6 months of age in a similar fashion to that previously published.[57] Briefly, scans were collected noninvasively using the Bioptigen System (Durham, NC). Because of the disorganization (rosette formation) in *Nrl*$^{-/-}$ retinas, autosegmentation could not be used to calculate thickness of retinal layers. Instead, outer nuclear layer (ONL) thickness was manually calculated as previously described.[57] Briefly, three lateral images (nasal to temporal) were collected: (1) 3 mm above the meridian crossing through the optic nerve head (ONH), (2) the meridian passing through the ONH, and (3) 3 mm below the ONH meridian. Three points were placed on identical locations on each meridian across samples. ONL thickness was measured at each point and values from treated and untreated *Nrl*$^{-/-}$*Gucy2e*$^{-/-}$ mice and *Nrl*$^{-/-}$ controls were compared with a paired *t*-test, with p-values of <0.05 considered significant.

Immunoblot

Mice were sacrificed, and retinas were prolapsed through a corneal incision, rapidly frozen, and stored at -80°C. Total retinal protein extracts were obtained from dissected retinas by sonication in 200 μl of sonication buffer (0.23 m*M* sucrose, 2 m*M* $MgCl_2$, 10 m*M* Tris-HCL, pH 7.5) containing inhibitors (Halt Protease and Phosphatase Inhibitor Cocktail; Thermo Scientific, Rockford, IL; cat #78410) at the supplier's recommended 1× concentration. Benzonase (Sigma-Aldrich, St. Louis, MO; cat #E1014) was added (0.1 μl) to each sample and the sample incubated for 15 min at 37°C. After incubation, 200 μl of 2×Laemmli buffer (BioRAD, Hercules, CA; cat #161-0737) was added. The samples were spun at 14,000 RPM for 5 min. A total volume of 20 μl per sample was loaded and electrophoresis was performed on 4–10% denaturing polyacrylamide gels and then transferred to polyvinylidene fluoride membrane using the Trans-Blot Turbo Transfer System (BioRad; cat #170-4155). Blots were incubated in Odyssey blocking buffer (Li-Cor, Lincoln, NE; cat #927-40000) for 1 hr to block nonspecific binding. Membranes were incubated overnight at 4°C with primary antibodies diluted in blocking buffer containing 0.2% Tween-20: rabbit anti-GC1 (1:1000; Santa Cruz, Biotechnology, Dallas, TX; cat #50512), rabbit anti-cone transducin (1:1000; Santa Cruz; cat #390), rabbit anti-rod transducin (1:1000; Santa Cruz; cat #389), rabbit anti-GC2 (1:5000, "L670"), rabbit anti-GCAP1 (1:30,000, "UW101"; kindly provided by Dr. Wolfgang Baehr), mouse-anti-RD3 (1:5; kindly provided by Dr. Robert Molday), rabbit anti-opsin red/green (1:1000; Millipore, Billerica, MA; cat #AB5405), rabbit anti-opsin, blue (1:1000; Millipore; cat #AB5407), rabbit anti-cone PDE6a′ (1:2000; "3184P" generously provided by Dr. Ramamurthy), or mouse anti-β-actin (1:1000; clone C4; Santa Cruz; cat #47778).

The following day, membranes were washed 4 times with 1×PBS and 0.1% Tween-20 for 10 min each at room temperature and were incubated for 1 hr with corresponding secondary antibodies: donkey anti-mouse (1:10,000; LiCor 680 RD; cat #926-68072), donkey anti-rabbit (1:10,000; Li-Cor 800CW; cat #923-32213), or donkey anti-goat

(1:10,000; LiCor 800CW; cat #923-32214) antibodies diluted in blocking buffer with 0.2% Tween-20. Membranes were washed 4× with 1×PBS and 0.1% Tween-20 for 10 min each at room temperature. Detection was performed using infrared imager (Li-Cor). β-actin was used as loading control. Protein from six $Nrl^{-/-}$ retinas, five untreated $Nrl^{-/-}Gucy2e^{-/-}$ retinas, and four AAV-treated $Nrl^{-/-}Gucy2e^{-/-}$ retinas was pooled, and each protein of interest was probed on three separate immunoblots. Protein expression was normalized to β-actin on individual blots. The average of those three values was then normalized against $Nrl^{-/-}$. Raw data obtained from each immunoblot are contained in Supplementary Table S1 (Supplementary Data are available online at www.liebertpub.com/hum).

Immunohistochemistry/microscopy

$Nrl^{-/-}Gucy2e^{-/-}$ mice treated with murine *Gucy2e* and $Nrl^{-/-}$ control mice were sacrificed at various ages depending on the stated purpose of each cohort and processed for IHC as previously described.[32,58] Briefly, eyes were enucleated, corneas punctured, and tissue placed in 4% PFA for 12 hr at 4°C. Cornea/lens were then removed and eyecups were transferred to 1× PBS followed by immersion in 30% sucrose for at least 2 hr at 4°C. Eyecups were then embedded in cryostat compound (Tissue-Tek OCT 4583; Sakura Finetek USA, Inc., Torrance, CA), quick-frozen in a bath of dry ice/EtOH, and serially sectioned at 12 μm with a cryostat (Leica CM3050 S). Retinal cross sections were stained with antibodies raised against retGC1 (rabbit polyclonal; Santa Cruz; sc50512; 1:200), M opsin (rabbit polyclonal; Chemicon; 1:200), and S opsin (Santa Cruz; sc14365; 1:200) or GCAP1 (rabbit polyclonal, "UW101," 1:5000; generously provided by Dr. Wolfgang Baehr, University of Utah). All primary antibodies were incubated overnight (retGC1 and GCAP1, 37°C; M opsin, 4°C; S opsin, 4°C). Alexafluor secondary antibodies were applied for 1 hr at room temperature. Mounting media containing 4′,6′-diaminio-2-phenylindole (DAPI) was applied and sections were then imaged using spinning disk confocal microscopy (Nikon Eclipse TE2000 microscope equipped with Perkin Elmer Ultraview Modular Laser System and Hamamatsu O-RCA-R2 camera), and 20× and 40× images of retGC1, M opsin, or S opsin were obtained using identical settings (exposure, gain, laser power) at each objective with Volocity 6.3 software (PerkinElmer, Waltham, MA).

RESULTS

Subretinal injection of AAV-*Gucy2e* fully restores retinal function to $Nrl^{-/-}Gucy2e^{-/-}$ mice over the long-term

Previously, it has been shown that gene replacement as late as ~P43 in the GCDKO mouse is sufficient to preserve photoreceptors.[34] Taken together with the expectation of treating post-adolescent patients in early clinical trials, we chose to treat $Nrl^{-/-}Gucy2e^{-/-}$ mice at approximately 41 days of age (i.e., P37–P45). In order to determine the effects of AAV-mediated retGC1 expression on retinal function, we performed ERG analysis out to 6 months of age. Full-spectrum photopic ERGs were performed at approximately 1 month and 2, 3, and 5 months postinjection (approximately 2, 3, 4, and 6 months of age) and compared with age-matched $Nrl^{-/-}$ controls. We observed robust ERG responses in the injected eyes of treated mice over the long-term, whereas untreated eyes exhibited no discernible wave forms (Fig. 1A). The amplitudes of full-spectrum cone responses in treated mice were significantly higher than $Nrl^{-/-}$ controls at 2 out of 4 time points (2 months, $p=0.036$; 3 months, $p=0.624$; 4 months, $p=0.754$; 6 months, $p=0.045$) (Fig. 1B). We further analyzed retinal function in treated and untreated $Nrl^{-/-}Gucy2e^{-/-}$ mice and age-matched $Nrl^{-/-}$ controls by utilizing ERG conditions designed to isolate M- and S-cone-driven responses. M- and S-cone ERGs were performed at 1 month and 5 months postinjection (Fig. 1C). M-cone responses in treated $Nrl^{-/-}Gucy2e^{-/-}$ mice were significantly higher than those found in age-matched $Nrl^{-/-}$ controls at both 2 and 6 months of age ($p<0.001$). S-cone responses in treated mice were not significantly higher than $Nrl^{-/-}$ controls at 2 months but became so by 6 months ($p=0.002$). Our results show that AAV treatment results in complete restoration of retinal function over the long-term in the $Nrl^{-/-}Gucy2e^{-/-}$ mouse.

Treatment restores useful vision to $Nrl^{-/-}Gucy2e^{-/-}$ mice over the long-term

To validate whether restoration of retinal function in treated $Nrl^{-/-}Gucy2e^{-/-}$ mice translated to gains in useful vision, optokinetic reflex testing was performed. Measurable visual acuity was observed in $Nrl^{-/-}Gucy2e^{-/-}$ mice treated with AAV-*Gucy2e* over the long-term (at least 6 months of age) (Fig. 2). Spatial frequency thresholds in treated $Nrl^{-/-}Gucy2e^{-/-}$ mice were significantly higher than those in age-matched $Nrl^{-/-}$ controls at both 3 and 6 months of age ($p<0.001$). $Nrl^{-/-}$ mice lost the ability to track at 6 months of age.

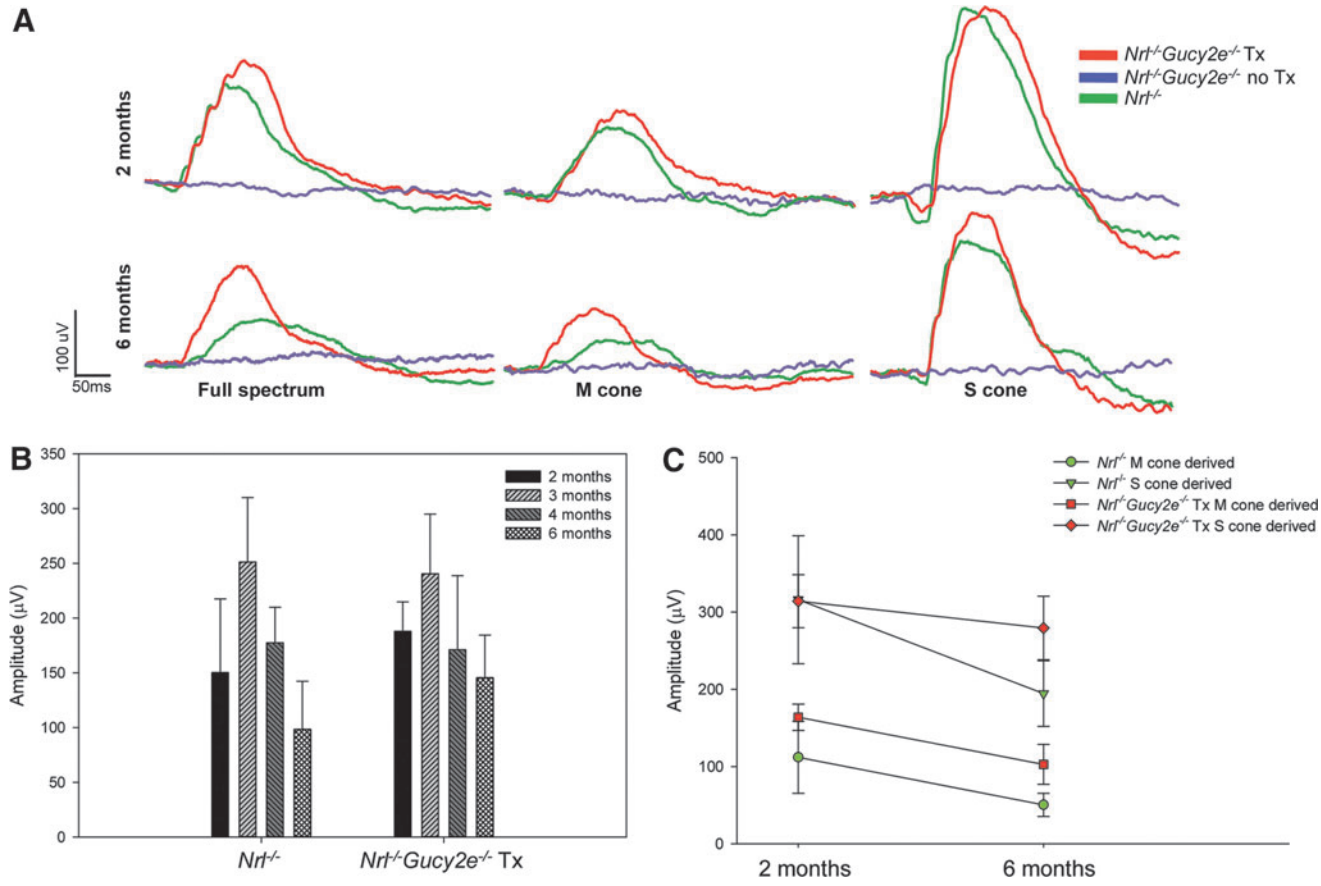

Figure 1. Long-term improvements in retinal function are achieved following AAV-*Gucy2e* treatment. Shown are representative cone ERG traces from treated and untreated $Nrl^{-/-}Gucy2e^{-/-}$ mice ($n=16$) and $Nrl^{-/-}$ controls ($n=8$) obtained under full-spectrum, M- or S-cone-isolating conditions at 2 and 6 months of age **(A)**, full-spectrum maximum cone b-wave amplitudes **(B)**, and M-/S-cone-derived maximum b-wave amplitudes **(C)** in treated and untreated $Nrl^{-/-}Gucy2e^{-/-}$ mice over time. Error bars in **(B)** and **(C)** represent ±1 SD.

Treated $Nrl^{-/-}Gucy2e^{-/-}$ mice exhibited a threshold decline between 3 and 6 months of age ($p<0.001$) (Fig. 2).

Functional efficiency of AAV-delivered retGC1

Guanylate cyclase activity assays were performed to evaluate the function of retGC1 enzyme encoded by AAV-delivered *Gucy2e* in the retinas of ~4-month-old treated and untreated $Nrl^{-/-}Gucy2e^{-/-}$ mice as well as age-matched $Nrl^{-/-}$ controls (Fig. 3). Because $Nrl^{-/-}$ mice lack retGC2 (Supplementary Fig. S1), there was no measurable retGC activity in untreated $Nrl^{-/-}Gucy2e^{-/-}$ retinas (Fig. 3).[45] As such, this assay measures the functional efficiency of only the enzyme expressed from the AAV vector. Interestingly, retGC activity was significantly higher in the AAV-treated $Nrl^{-/-}Gucy2e^{-/-}$ retinas relative to $Nrl^{-/-}$ controls ($p<0.001$). The $Ca^{2+}{}_{1/2}$ in treated retinas was similar to that in $Nrl^{-/-}$ controls (0.08 μM), indicating that the calcium sensitivity of AAV-mediated retGC1 was normal. This result is consistent with

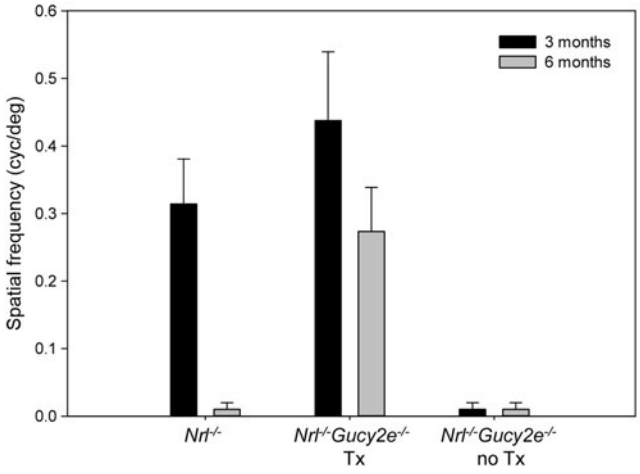

Figure 2. Visually guided behavior testing (optokinetic reflex) reveals long-term restoration of useful vision after AAV-*Gucy2e* treatment. Shown are average cone-mediated spatial frequency thresholds in treated and untreated $Nrl^{-/-}Gucy2e^{-/-}$ mice ($n=16$) and $Nrl^{-/-}$ controls ($n=8$) at 3 (black bars) and 6 (gray bars) months of age. Error bars represent ±1 SD.

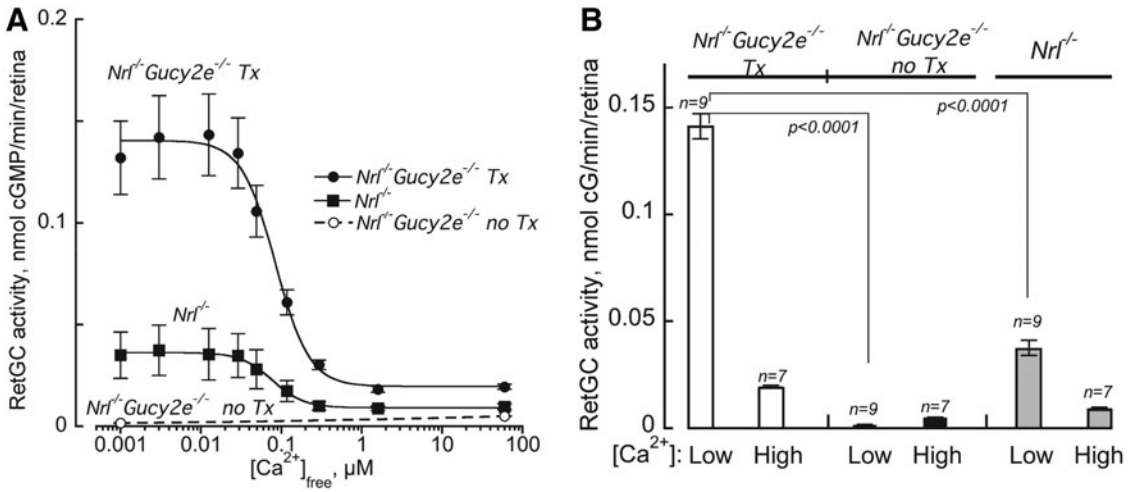

Figure 3. Functional efficiency of AAV-mediated retGC1 *in vivo*. Shown are guanylate cyclase activities (mean ± SE) in AAV-*Gucy2e*-treated and untreated $Nrl^{-/-}Gucy2e^{-/-}$ mice, and $Nrl^{-/-}$ controls titrated with different free Ca^{2+} at 1 m*M* free Mg^{2+} **(A)** and retGC1 activities in all cohorts (mean ± SE) in low (< 0.01 μM) versus high (2–60 μM) Ca^{2+} at saturating Mg^{2+} **(B)**.

our previous finding that calcium sensitivity of AAV-mediated retGC1 in treated GCDKO mice was also normal.[34]

"Supernormal" treatment effects are not the result of retGC1 insufficiency in $Nrl^{-/-}$ cones

Previous proof-of-concept studies evaluating the effects of retGC1 replacement in GC1KO and GCDKO mice revealed that only partial ERG recovery was possible, with treated ERG responses reaching, at best ~50–60% of WT, despite the vector-mediated retGC1 having identical calcium sensitivity and catalytic efficiency.[32–34,59] In contrast, the current study shows that both retinal function and visual acuity were significantly better in AAV-treated $Nrl^{-/-}Gucy2e^{-/-}$ mice than in $Nrl^{-/-}$ controls. As previously mentioned, functional efficiency of retGC1 was greater in the AAV-treated $Nrl^{-/-}Gucy2e^{-/-}$ mice than in age-matched $Nrl^{-/-}$ controls. This led us to question whether $Nrl^{-/-}$ mice simply express less retGC1 per cone photoreceptor than WT cones and/or are amenable to its "overexpression" by AAV. We therefore investigated the consequences of retGC1 supplementation via AAV on cone function in P35-treated $Nrl^{-/-}$ mice. Full-spectrum, M- and S-cone-derived ERG responses recorded 1 month postinjection reveal that responses in treated eyes (under all conditions) were not improved (Supplementary Fig. S2). IHC analysis of retinal cross sections from treated and untreated $Nrl^{-/-}$ mice reveals no visible difference in the level of retGC1 expression (data not shown). Our results indicate that the "supernormal" responses seen in the treated $Nrl^{-/-}Gucy2e^{-/-}$ mice are unlikely the result of higher retGC1 expression on a per-cone basis.

In vivo retinal structure of $Nrl^{-/-}Gucy2e^{-/-}$ mice and treatment efficacy

OCT was performed in 6-month-old treated and untreated $Nrl^{-/-}Gucy2e^{-/-}$ mice and age-matched $Nrl^{-/-}$ controls to quantify cone cell densities. Average ONL thickness measurements from identical retinal locations were calculated and averaged for all cohorts. At 6 months of age, ONLs of untreated $Nrl^{-/-}Gucy2e^{-/-}$ mice were 28% thinner than $Nrl^{-/-}$ controls ($p < 0.001$), indicating that, as in other models of retGC1 deficiency, lack of the cyclase results in cone degeneration (Fig. 4A).[32,34,36,60] AAV-*Gucy2e* treatment resulted in significant cone preservation in $Nrl^{-/-}Gucy2e^{-/-}$ retinas relative to that seen in untreated contralateral controls ($p < 0.001$) with ONLs on average being 35% thicker (Fig. 4A). Our measurements also revealed that ONLs of treated mice were 10% thicker than age-matched $Nrl^{-/-}$ controls. This result was statistically significant ($p = 0.022$). Representative OCT scans from each cohort are shown in Supplementary Fig. S3. To examine whether cone degeneration/preservation followed a spatial pattern, we analyzed ONL thicknesses separately in superior versus inferior retinas of all cohorts (Fig. 4B). Six-month-old $Nrl^{-/-}$ control mice had significantly fewer cones in their inferior versus superior retinas ($p = 0.036$). The same was true in untreated $Nrl^{-/-}Gucy2e^{-/-}$ mice ($p = 0.031$). Relative to untreated $Nrl^{-/-}$

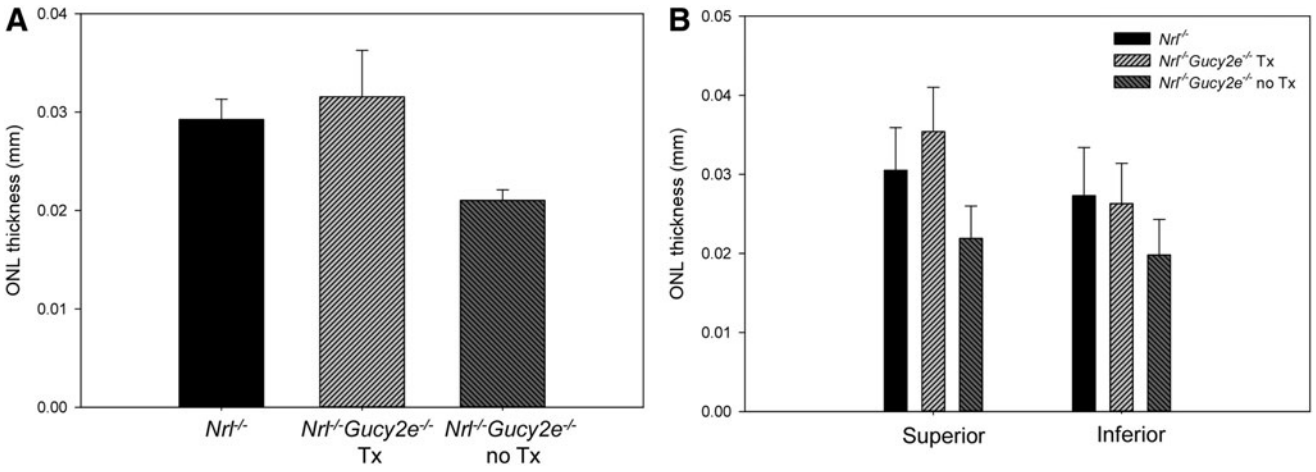

Figure 4. Cones are preserved in AAV-*Gucy2e*-treated $Nrl^{-/-}Gucy2e^{-/-}$ mice over the long-term. Shown are outer nuclear layer thicknesses derived from identical retinal regions of AAV-*Gucy2e*-treated and untreated $Nrl^{-/-}Gucy2e^{-/-}$ mice, and $Nrl^{-/-}$ controls at 6 months of age. Values from eight points encompassing all retinal regions are plotted **(A)** as well as those from superior vs. inferior retina **(B)**. Error bars represent ± 1 SD.

$Gucy2e^{-/-}$ mice, significant cone preservation ($p < 0.001$) was achieved in both the superior and inferior retinas of AAV-treated mice. Cone preservation was achieved to a greater extent in the superior retinas of treated mice. There were significantly more cones in the superior retinas of treated $Nrl^{-/-}Gucy2e^{-/-}$ mice relative to $Nrl^{-/-}$ controls ($p < 0.001$), while the number of cones in the inferior retinas of each strain did not significantly differ ($p = 0.474$). Previous results indicate that inferior cones of the $Nrl^{-/-}$ retina have an increased susceptibility to death, as evidenced by the earlier and higher levels of microglial activation in this region.[61]

retGC1 deficiency until at least postnatal day 35 is required to confer supernormal functional improvements to AAV-treated $Nrl^{-/-}Gucy2e^{-/-}$ mice

The modest but statistically significant increase in ONL thickness exhibited in 6-month-old treated $Nrl^{-/-}Gucy2e^{-/-}$ compared with age-matched $Nrl^{-/-}$ retina suggests that the absence of retGC1 lasting at least up to P35 has a structurally protective effect. This early but transient absence of cyclase "poises" the $Nrl^{-/-}Gucy2e^{-/-}$ retina for treatment, ultimately allowing for thicker ONLs (Fig. 4), higher retGC1 activity (Fig. 3), ERG (Fig. 1), and behavioral responses (Fig. 2) in 6-month-old treated mice relative to $Nrl^{-/-}$ controls. However, long-term absence of retGC1 does result in thinning as evidenced by comparing the untreated $Nrl^{-/-}Gucy2e^{-/-}$ mice relative to age-matched $Nrl^{-/-}$ controls, or the treated $Nrl^{-/-}Gucy2e^{-/-}$ mice (Fig. 4). We hypothesized that the observed structural protection can be, for a reason presently unknown, related to retGC1 deficiency in early development. To investigate this, we subretinally injected AAV-*Gucy2e* into younger (P18) $Nrl^{-/-}Gucy2e^{-/-}$ mice and tested whether supernormal retinal function was achieved at 1 month postinjection (Fig. 5). Consistent with our hypothesis, ERG responses (full-spectrum, M- and S-cone-driven) were now lower in treated $Nrl^{-/-}Gucy2e^{-/-}$ mice than in $Nrl^{-/-}$ controls, suggesting that introduction of retGC1 into $Nrl^{-/-}Gucy2e^{-/-}$ cones at this early time point converted them phenotypically back into $Nrl^{-/-}$ cones that were no longer protected.

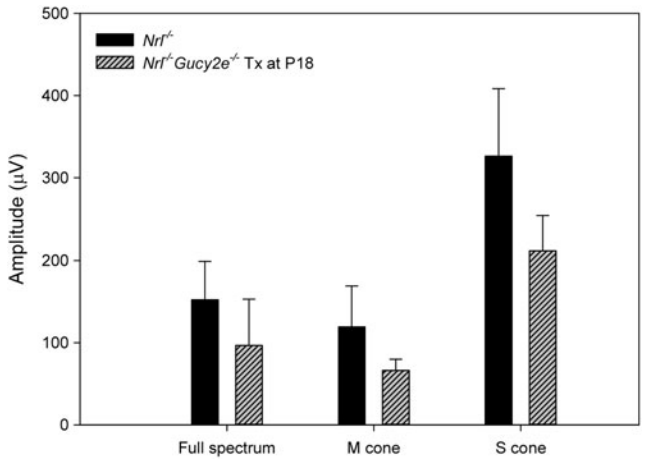

Figure 5. Retinal function in $Nrl^{-/-}Gucy2e^{-/-}$ mice treated at P18 with AAV-*Gucy2e*. Shown are average maximum cone b-wave amplitudes obtained under full-spectrum, M- or S-cone-isolating conditions in treated $Nrl^{-/-}Gucy2e^{-/-}$ mice ($n = 7$) (gray, striped bars) and $Nrl^{-/-}$ controls ($n = 9$) (black bars) at 2 months of age. Error bars represent ± 1 SD.

Effect of AAV treatment on the expression of relevant phototransduction proteins

Immunoblots were performed to evaluate relative expression of various phototransduction proteins within pooled whole retinas of treated ($n=4$) and untreated ($n=5$) $Nrl^{-/-}Gucy2e^{-/-}$ mice and age-matched $Nrl^{-/-}$ controls ($n=6$) (Fig. 6). Each protein was probed on three separate immunoblots and representative images are shown in Fig. 6A. Not surprisingly, retGC1 expression was absent from the untreated $Nrl^{-/-}Gucy2e^{-/-}$ retinas but was restored to the level seen in age-matched $Nrl^{-/-}$ retinas following treatment (Fig. 6A). Consistent with the enzyme activity assays (Fig. 3) and previous reports, retGC2 expression was absent from all strains on the $Nrl^{-/-}$ background

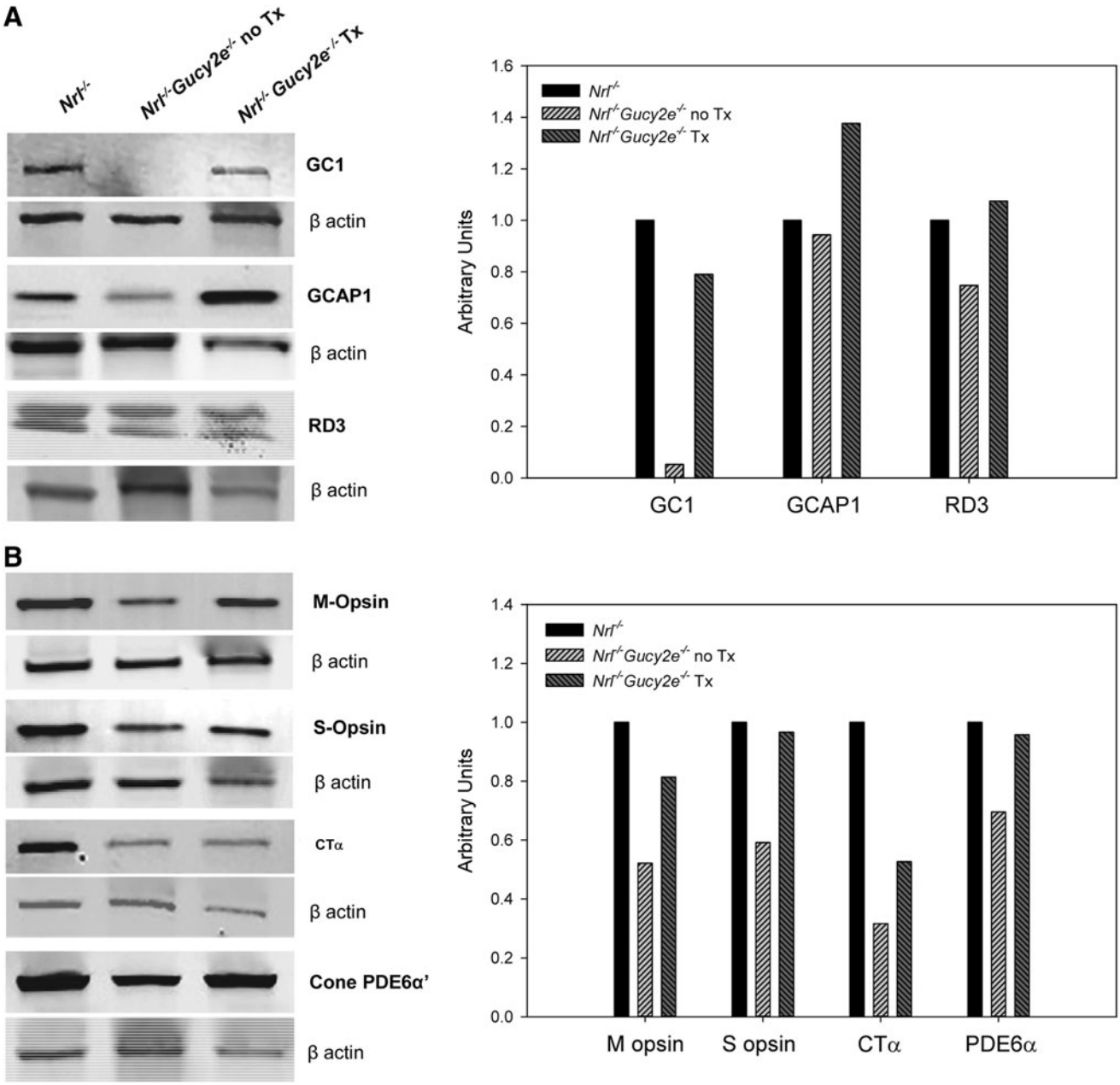

Figure 6. Expression of retGC1 and other relevant phototransduction proteins in pooled retinas of treated ($n=4$) and untreated ($n=5$) $Nrl^{-/-}Gucy2e^{-/-}$ mice and $Nrl^{-/-}$ controls ($n=6$). Shown are semiquantitative immunoblots from whole retinal extracts probed with antibodies against retGC1, its biochemical partner GCAP1, and trafficking partner, RD3 **(A)** and relevant cone phototransduction proteins, M opsin, S opsin, cone transducin (CTα), and cone PDE6α' **(B)**. β-actin was used as loading control. Each protein was probed on three separate immunoblots and representative images are shown in **(A)**. For densitometric analysis, expression of each protein was first normalized to β-actin on each blot. These ratios were averaged and values were then normalized to $Nrl^{-/-}$ controls.

(Supplementary Fig. S1).[45] A comparison of both retGC2 and rod transducin expression in rod-dominant C57BL/6 and GCDKO retinas alongside those on the $Nrl^{-/-}$ background revealed the absence of both proteins in the cone-dominant retinas (Supplementary Fig. S1). Interestingly, GCAP1, whose preferential target *in vivo* is retGC1, was expressed at comparable levels in untreated $Nrl^{-/-}$ *Gucy2e*$^{-/-}$ and $Nrl^{-/-}$ control retinas (Fig. 6A).[14] This starkly contrasts previous reports demonstrating downregulation of GCAP1 in other models of retGC1 deficiency.[36,59,62] Unlike all other proteins analyzed, which approached normal $Nrl^{-/-}$ control levels following AAV-*Gucy2e* treatment, GCAP1 expression was ~25% higher in the treated $Nrl^{-/-}$ *Gucy2e*$^{-/-}$ retinas relative to $Nrl^{-/-}$ controls (Fig. 6A).

Expression of RD3, a protein required for the transport of retGC1 to photoreceptor outer segments,[63] was downregulated in untreated mice and returned to normal levels following treatment (Fig. 6A). RD3's appearance on immunoblot (i.e., a doublet) was identical to that previously shown using the same antibody a doublet.[64,65] Both M and S opsin were downregulated in untreated $Nrl^{-/-}$ *Gucy2e*$^{-/-}$ retinas and also returned to normal following treatment (Fig. 6B). The same was true of cone PDE6α′, another protein thought to traffic with retGC1 to the outer segments.[66] The alpha subunit of cone transducin (CTα) was also downregulated in untreated $Nrl^{-/-}$*Gucy2e*$^{-/-}$ retinas. AAV-*Gucy2e* treatment promoted higher levels of expression but, unlike the other proteins examined, CTα expression was only restored to approximately half that seen in $Nrl^{-/-}$ controls (Fig. 6B).

AAV treatment of $Nrl^{-/-}$*Gucy2e*$^{-/-}$ restores expression of M and S opsin to cone outer segments

To evaluate localization of AAV-mediated retGC1 and opsin proteins, we analyzed frozen retinal cross sections from treated and untreated $Nrl^{-/-}$ *Gucy2e*$^{-/-}$ mice alongside $Nrl^{-/-}$ controls at 6 months. As reported for other models of LCA1, AAV-mediated retGC1 expression was restricted to photoreceptor outer segments in subretinally treated $Nrl^{-/-}$*Gucy2e*$^{-/-}$ mice[32–34,58] (Fig. 7A). Consistent with *in vivo* analysis, DAPI-stained cross sections reveal higher cone densities in treated $Nrl^{-/-}$ *Gucy2e*$^{-/-}$ and $Nrl^{-/-}$ retinas relative to that seen in untreated $Nrl^{-/-}$*Gucy2e*$^{-/-}$ mice (Fig. 7A and B). M opsin expression was more apparent in treated $Nrl^{-/-}$*Gucy2e*$^{-/-}$ retinas than in untreated contralateral controls or $Nrl^{-/-}$ retinas. S opsin expression was similar in treated and $Nrl^{-/-}$ control mice, whereas it was notably reduced in untreated $Nrl^{-/-}$*Gucy2e*$^{-/-}$ retina (Fig. 7B).

GCAP1 localization is altered on the $Nrl^{-/-}$ background

Intrigued by the finding that GCAP1 was not downregulated in untreated $Nrl^{-/-}$*Gucy2e*$^{-/-}$ mice, as it is in all other models of retGC1 deficiency previously evaluated, we analyzed its expression in retinal cross sections (Fig. 8). Unlike C57BL/6 retinas where GCAP1 expression is seen exclusively in the photoreceptor IS/OS and synaptic termini, its localization is altered in $Nrl^{-/-}$ controls and untreated and treated $Nrl^{-/-}$*Gucy2e*$^{-/-}$ mice. High-magnification images reveal that GCAP1 staining is found throughout the ONL of all three cohorts. While it is more difficult to decipher OS morphology in mice on the $Nrl^{-/-}$ background, we noted brighter punctate areas of GCAP1 expression in OS of treated $Nrl^{-/-}$*Gucy2e*$^{-/-}$ mice (denoted by white arrows) that were not typical for untreated mice or $Nrl^{-/-}$ controls (Fig. 8).

Retinal function is restored to $Nrl^{-/-}$ *Gucy2e*$^{-/-}$ mice treated at postnatal day 45 with a clinically relevant vector, AAV5-hGRK1-*GUCY2D*, expressing human retGC1

Gene therapy for color blindness has proven successful in primate using an AAV5 vector.[67] Furthermore, we have shown that AAV5 and the hGRK1 promoter drive efficient transgene expression in both foveal and parafoveal cones of macaque following subretinal injection.[52] Given that the locus of dysfunction in LCA1 patients is the fovea, a clinical vector for LCA1 comprising an AAV5-based capsid containing the hGRK1 promoter driving the human retGC1 gene, *GUCY2D*, would be warranted. Demonstration that AAV5-hGRK1-*GUCY2D* can restore retinal function to a disease model within a translatable therapeutic window would be highly advantageous. Here, we asked whether the $Nrl^{-/-}$*Gucy2e*$^{-/-}$ mouse model was amenable to treatment with species nonspecific retGC1, that is, *GUCY2D*, in the adult mouse. Full-spectrum ERG analysis of $Nrl^{-/-}$*Gucy2e*$^{-/-}$ mice treated at P40 with AAV5-hGRK1-*GUCY2D* revealed robust restoration of cone function at ~2 months of age (Fig. 9A). Responses in treated eyes were not significantly different from age-matched $Nrl^{-/-}$ controls ($p = 0.366$). Cones treated with AAV5-hGRK1-*GUCY2D* had significantly lower responses than those treated with AAV8(733)-hGRK1-*Gucy2e* ($p = 0.018$). Based on our unpublished work using the human transgene and the relative strength of AAV5 and AAV8(733) in

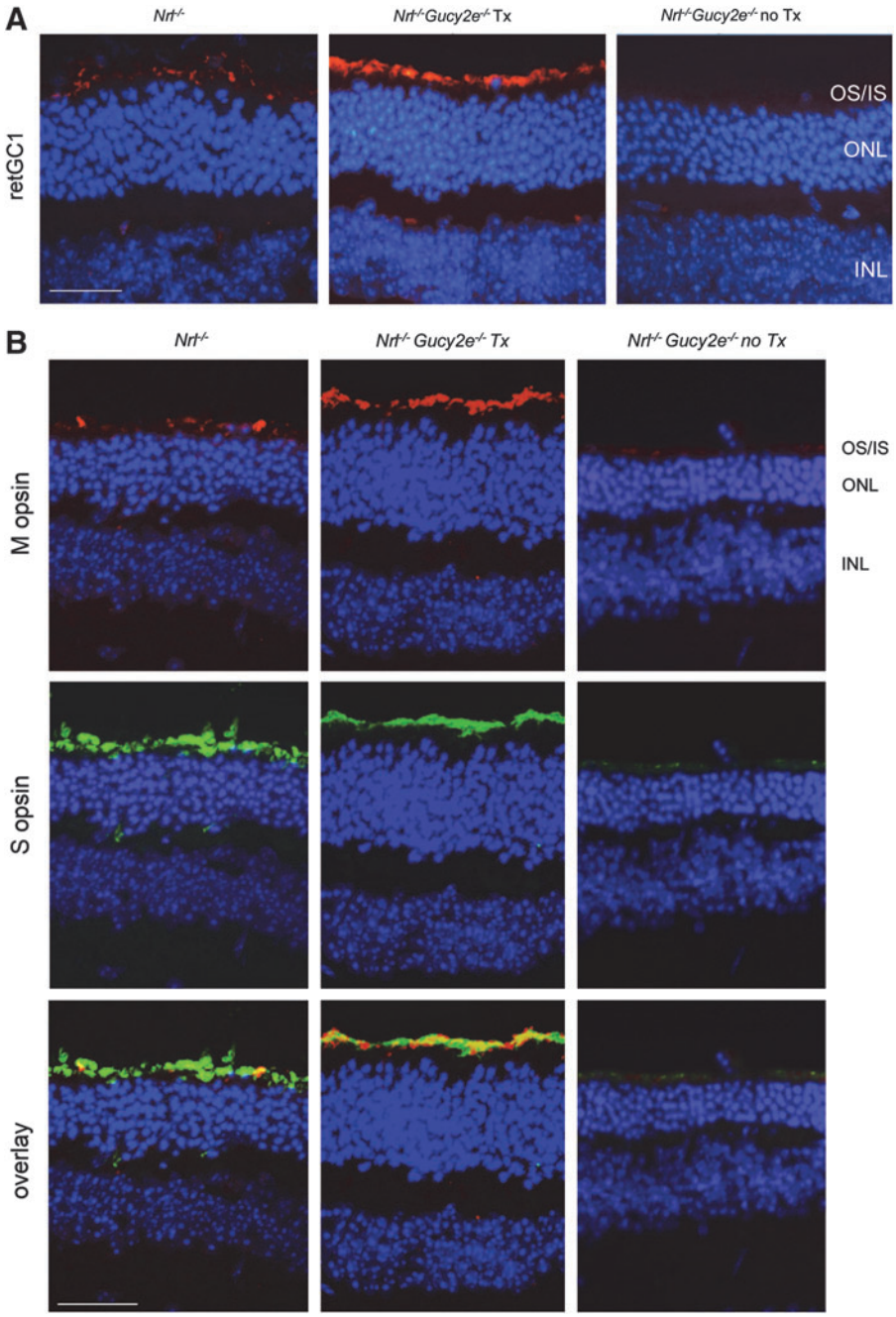

Figure 7. Expression of retGC1 and cone opsins in retinal cross sections of AAV-*Gucy2e*-treated and untreated $Nrl^{-/-}$ *Gucy2e*$^{-/-}$ mice and $Nrl^{-/-}$ controls. Shown are retGC1 (red) **(A)** M opsin (red) and S opsin (green) **(B)** expression in representative 40× images from all three cohorts at 6 months of age. All sections were counterstained with DAPI (blue). Scale bars = 50 μm.

murine photoreceptors, we believe that this difference was attributed both to serotype differences and the nature of the delivered cDNA (human vs. murine).[33] The full-spectrum response in AAV5-hGRK1-*GUCY2D*-treated eyes was undetectable by 6 months of age (Fig. 9A). However, isolation of the S-cone-mediated ERG revealed maintenance of retinal function at this time point (Fig. 9B).

DISCUSSION

We have shown that subretinal delivery of an AAV8(733) vector containing the photoreceptor-specific human rhodopsin kinase promoter is capable of restoring retGC1 expression to the cone-only $Nrl^{-/-}$*Gucy2e*$^{-/-}$ mouse. Notably, gene replacement resulted in full and long-term restoration of retinal function and visually guided

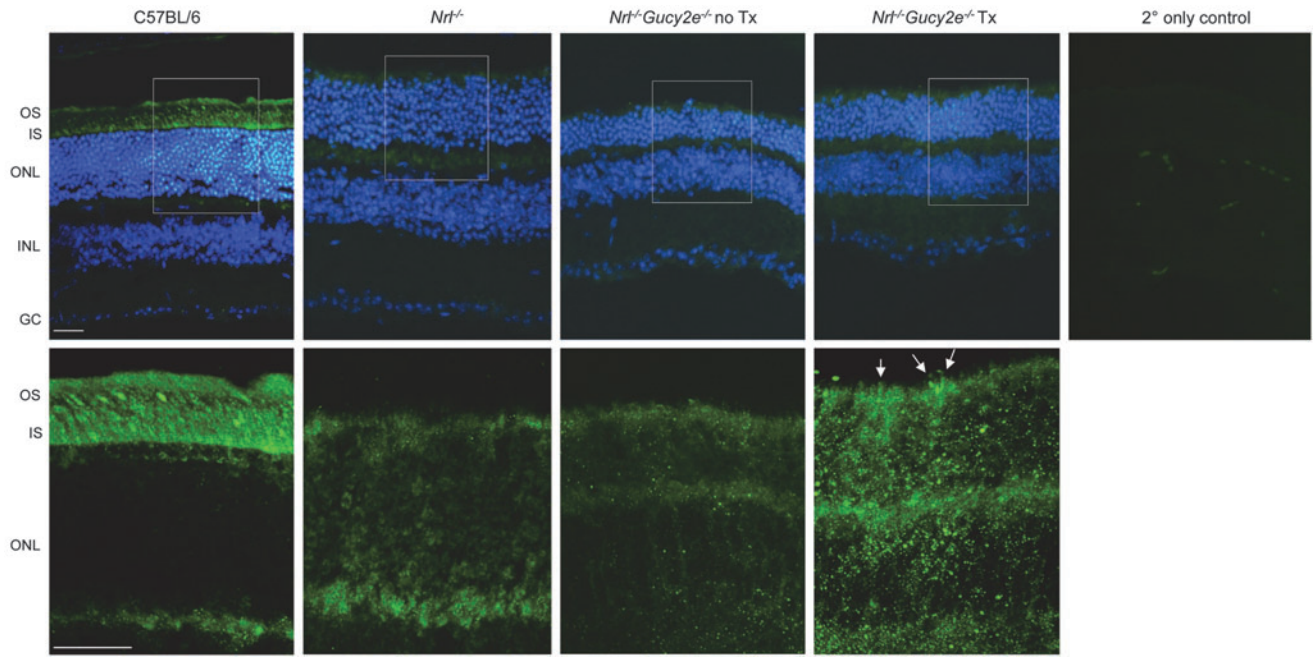

Figure 8. GCAP1 expression in representative retinal cross sections of AAV-*Gucy2e*-treated and untreated $Nrl^{-/-}$ *Gucy2e*$^{-/-}$ mice, C57BL/6 WT, and $Nrl^{-/-}$ controls. Shown in the top row are GCAP1 (green) expression in 20× images counterstained with DAPI (blue) and a secondary only control. White boxes in 20× images are magnified in the bottom row, where only GCAP1 (green) is shown. White arrows in the high-magnification image of AAV-treated $Nrl^{-/-}$ *Gucy2e*$^{-/-}$ mice denote cone outer segments with more obvious GCAP1 staining. GC, ganglion cells; INL, inner nuclear layer; IS, inner segments; no Tx, no treatment; ONL, outer nuclear layer; OS, outer segments; Tx, treatment. Scale bars = 30 μm.

behavior. Cone photoreceptors were preserved with densities in AAV-treated mice surpassing those found in $Nrl^{-/-}$ controls at 6 months of age. Relevant phototransduction proteins such as M opsin, S opsin, cone transducin, and PDE6α', all of which were downregulated in untreated mice, were upregulated following treatment. Additionally, we show that an AAV5 vector containing human retGC1 cDNA is capable of rescuing cone function following treatment of adult $Nrl^{-/-}$*Gucy2e*$^{-/-}$ mice.

Several interesting observations were made over the course of this study. First, retinal function as measured by ERG was equal to or better in the

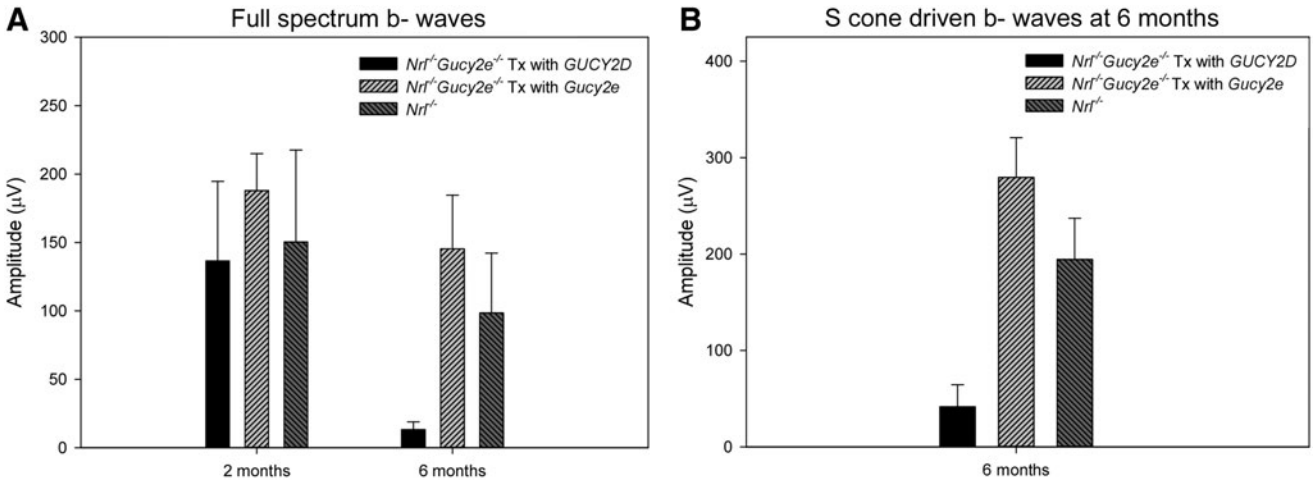

Figure 9. Retinal function is restored to $Nrl^{-/-}$*Gucy2e*$^{-/-}$ mice following treatment at P40 with AAV5-hGRK1-*GUCY2D*. Shown are full-spectrum maximum cone b-wave amplitudes at 2 and 6 months of age **(A)** and S-cone-derived maximum b-wave amplitudes at 6 months **(B)** in treated and untreated $Nrl^{-/-}$*Gucy2e*$^{-/-}$ mice (n=7) and $Nrl^{-/-}$ controls (n=8). Error bars represent ±1 SD.

treated $Nrl^{-/-}Gucy2e^{-/-}$ mice relative to age-matched $Nrl^{-/-}$ controls. This is in stark contrast to previous results where only partial recovery of retinal function was observed ($\sim$50–60% of WT) in GC1 KO and GCDKO mice using the same vector.[32,33,59] We also found that guanylate cyclase activity in AAV-treated $Nrl^{-/-}Gucy2e^{-/-}$ retinas was substantially higher than that seen in $Nrl^{-/-}$ controls. Because $Nrl^{-/-}$ retinas contain fewer total photoreceptors and because their outer segments are significantly shorter/contain fewer discs, it was not surprising that retGC activity in this strain is lower than that reported in WT mice.[34,45] It was also expected that, because $Nrl^{-/-}$ mice lack retGC2, that untreated $Nrl^{-/-}Gucy2e^{-/-}$ mice would have no enzyme activity, as we indeed found. What was not expected was that AAV-*Gucy2e* treatment of $Nrl^{-/-}Gucy2e^{-/-}$ mice resulted in substantially higher guanylate cyclase activity than that seen in age-matched $Nrl^{-/-}$controls. This prompted us to speculate whether retGC1 expression was limiting in $Nrl^{-/-}$ controls. In other words, perhaps cones in treated $Nrl^{-/-}Gucy2e^{-/-}$ mice simply expressed more retGC1 per cone than in $Nrl^{-/-}$ mice. However, two observations suggested that this was not the case. First, immunoblot revealed that retGC1 was expressed at slightly lower levels in treated $Nrl^{-/-}Gucy2e^{-/-}$ retinas relative to $Nrl^{-/-}$ controls, even with the former containing a thicker ONL. Second, attempts to overexpress retGC1 in $Nrl^{-/-}$ mice via AAV did not lead to improvements in retinal function. Therefore, insufficiency of retGC1 is not the basis for the observed difference in activity. Additionally, we do not believe that the reason for higher retGC1 activity in treated $Nrl^{-/-}Gucy2e^{-/-}$ mice relative to $Nrl^{-/-}$ controls is simply a function of higher cone densities in the former. The relative ONL thickness difference between treated $Nrl^{-/-}Gucy2e^{-/-}$ and $Nrl^{-/-}$ mice at 6 months is modest ($\sim$10%). Taken together with the fact that the area of mouse retina transduced by subretinally delivered AAV rarely exceeds 80%, it is hard to envision that there are enough additional photoreceptors expressing retGC1 in treated $Nrl^{-/-}Gucy2e^{-/-}$ mice to account for this difference in cyclase activity. The results of the immunoblot for retGC1 again argue that this is not the case. This leads us to GCAP1 and the role that it may be playing in determining the difference in cyclase activity.

The impact of retGC1 deficiency on GCAP1 expression in $Nrl^{-/-}Gucy2e^{-/-}$ mice is different from all previous LCA1 models studied to date. In rod-dominant GC1KO and GCDKO mice, GCAP1 expression is severely downregulated in the absence of retGC1.[33,34,60] In the cone-dominant GUCY1*B chicken, GCAP1 is nearly absent from predegenerate retinas.[61] Here we found, via immunoblot, that the absence of retGC1 in $Nrl^{-/-}Gucy2e^{-/-}$ retina had little effect on GCAP1 expression. Furthermore, unlike most phototransduction proteins evaluated, which approached normal ($Nrl^{-/-}$) levels following AAV-treatment, GCAP1 was overexpressed. This contrasts previous studies where GCAP1 levels were restored to, but not above, WT levels.[33,34] These differences prompted our analysis of its localization in retinal cross sections. As previous studies have shown, GCAP1 localized very distinctly to photoreceptor inner and outer segments (IS/OS) and synaptic termini of C57BL/6 mice.[14,34,36] This pattern was altered in $Nrl^{-/-}$ cones, with staining spread diffusely throughout the remnant OS, ONL, and synaptic termini. Expression was similarly diffuse in cross sections of untreated and treated $Nrl^{-/-}Gucy2e^{-/-}$ mice, but in treated eyes, punctate foci of higher GCAP1 expression were noted in OS. This led us to speculate whether reduced availability of GCAP1 in the OS of $Nrl^{-/-}$ cones (i.e., reduced availability of a functional GCAP1/retGC1 complex) was the reason for the low observed retGC1 activity in these retinas relative to WT, despite its high abundance in immunoblots of whole retina.[34,45] Supporting this is the observation that supplementation of GCAP1 protein to the $Nrl^{-/-}$ retinal extract in the guanylate cyclase activity assay results in at least a 2-fold increase in retGC1 activity, comparable to what was observed in treated $Nrl^{-/-}Gucy2e^{-/-}$ mice (Dizhoor et al., unpublished results).

Why is GCAP1 distribution altered in $Nrl^{-/-}$ and $Nrl^{-/-}Gucy2e^{-/-}$ mice? GCAP1 localization on the $Nrl^{-/-}$ background is likely to be affected by the physiological state of photoreceptors in this unique retina. Several lines of evidence suggest that oxygen stress in the $Nrl^{-/-}$ retina is higher than that in WT.[42,61] Oxidative stress causes rapid increases in Ca^{2+} concentration in the cytoplasm of diverse cell types, including cones.[68,69] Prolonged high Ca^{2+}, which comes from both the extracellular environment as well as intracellular stores, can lead to apoptotic death of photoreceptors, a pathway that has been implicated in inherited retinal disease.[69,70] It is reasonable to assume that oxidative stress in $Nrl^{-/-}$ cones could lead to abnormal increases in intracellular Ca^{2+}. In its Ca^{2+}-bound form, GCAP1 inhibits retGC1.[56,71] We therefore hypothesize that the Ca^{2+}-free form of GCAP1, rather than GCAP1 alone, is limiting based on its robust expression in untreated $Nrl^{-/-}Gucy2e^{-/-}$ mice (immunoblot and IHC of retinal cross sections). So, why isn't GCAP1 downregulated in

Nrl$^{-/-}$*Gucy2e*$^{-/-}$ mice as it is in other models of LCA1, like the GUCY1*B chicken and GC1KO and GCDKO mouse? While these models ultimately suffer photoreceptor death, which is believed to result from retGC1 deficiency, leading to chronic hyperpolarization, cGMP accumulation, and/or Ca^{2+} depletion, they all possess a normal complement of rods and cones early in development. This early retinal homeostasis likely does not induce hyperoxia as seen in *Nrl*$^{-/-}$ mice. It is known that Ca^{2+} stabilizes GCAP1 by altering its tertiary structure and increasing folding stability.[72,73] At saturating Ca^{2+} concentrations, GCAP1 can dimerize.[72] One could suggest that hyperoxia in cones of *Nrl*$^{-/-}$ and *Nrl*$^{-/-}$*Gucy2e*$^{-/-}$ mice leads to increases in cytosolic Ca^{2+} in the inner segment that bind and stabilize GCAP1. It is tempting to further speculate that Ca^{2+}-bound GCAP1 is trafficked less efficiently to cone outer segments and/or is degraded in the inner segment less effectively. While there is currently no direct evidence to support this hypothesis, it is a possible explanation for the relatively high GCAP1 expression detected in immunoblots and altered distribution in retinas of *Nrl*$^{-/-}$ and *Nrl*$^{-/-}$*Gucy2e*$^{-/-}$ mice.

Another intriguing observation was the apparent protective effect conferred by the absence of retGC1 during the first ~40 days in the *Nrl*$^{-/-}$ retina. The role of retGC1 is to produce most of the cGMP required to open cyclic nucleotide gated channels and allow Na^+ and Ca^{2+} influx into photoreceptors.[1] Under hyperoxic conditions resulting in high intracellular Ca^{2+} in *Nrl*$^{-/-}$ cones, it is not unreasonable to expect that retGC1 deficiency could have a transient protective effect by keeping cGMP-gated channels closed and preventing further increases in Ca^{2+}. Protection of photoreceptors following shRNA-mediated knockdown of retGC1 in the *PDE6b*^{H620Q} mutant mouse was reported to occur via a related mechanism.[74] Yet somehow this protective effect is not sustained after the *Nrl*$^{-/-}$ retina reorganizes/stabilizes (after 4 months), after which the detrimental effects of retGC1 deficiency would manifest as in other models of LCA1.[61] We speculate that the lowering of cGMP/prevention of additional Ca^{2+} influx into cones of young *Nrl*$^{-/-}$*Gucy2e*$^{-/-}$ mice slowed their rate of loss relative to that seen in *Nrl*$^{-/-}$ controls during a period when the latter undergoes rapid cone loss/reorganization. The single-stranded AAV vector used in this study was delivered ~P40 mediating appreciable levels of retGC1 expression ~3 weeks postinjection. In 2-month-old *Nrl*$^{-/-}$*Gucy2e*$^{-/-}$ mice, it is likely that a higher number of cones were therefore available for transduction. We speculated that retGC1 deficiency would exert its protective effects only if sustained over a significant period of time during which the *Nrl*$^{-/-}$ retina is exposed to hyperoxic stress (before 4 months of age). In other words, if retGC1 was supplemented too early, the *Nrl*$^{-/-}$*Gucy2e*$^{-/-}$ mouse would phenotypically revert back to the *Nrl*$^{-/-}$ state.

To test this, we introduced retGC1 back into *Nrl*$^{-/-}$*Gucy2e*$^{-/-}$ cones at P18. Indeed, earlier treatment failed to confer supernormal ERG responses to treated *Nrl*$^{-/-}$*Gucy2e*$^{-/-}$ mice. It is likely that retGC1 supplementation at this early age further contributed to Ca^{2+} toxicity, causing accelerated death of photoreceptors and reduced overall retinal function akin to what occurs in the *Nrl*$^{-/-}$ retina. The ~23% reduction in ERG response in P18-treated *Nrl*$^{-/-}$*Gucy2e*$^{-/-}$ mice is consistent with injection-related damage, suggesting that retinal function in treated mice and *Nrl*$^{-/-}$ controls was identical. Previous studies show that retinal changes on the *Nrl*$^{-/-}$ background affect more than just photoreceptors.[61] By 6 months of age, *Nrl*$^{-/-}$ mice exhibit optic nerve palor, indicating that degeneration of ganglion cells has also occurred. Our finding that 6-month-old *Nrl*$^{-/-}$ mice lack visually guided behavior complements this finding and highlights the need for caution when using *Nrl*$^{-/-}$ mice in visually guided behavior experiments at advanced ages. Via mechanisms that remain to be elucidated, we show that early and transient retGC1 deficiency also protected the inner retina, allowing for maintenance of useful vision over the long-term.

It is worth considering our findings in the context of recent studies evaluating other mutations on the *Nrl*$^{-/-}$ background. The *Nrl*$^{-/-}$*Aipl1*$^{-/-}$ mouse was used to investigate the mechanism of cone cell death in *AIPL1* LCA.[46] Investigators found that the Aipl protein was essential for the stability of retGC1 in cones and that, in its absence, retGC1 trafficking was defective, cGMP was decreased, and cones were lost much more rapidly than in *Nrl*$^{-/-}$ controls.[46] Authors speculated that cone death in the *Nrl*$^{-/-}$*Aipl1*$^{-/-}$ mouse and *AIPL1*-LCA patients may be because of a loss of retGC1 function. However, cone degeneration in P200 *Nrl*$^{-/-}$*Aipl1*$^{-/-}$ mice was much more pronounced than that seen in *Nrl*$^{-/-}$*Gucy2e*$^{-/-}$ mice at a similar age. This suggests that Aipl1 has an additional function in cones, which is not surprising given the better cone preservation in *GUCY2D* LCA1 patients versus those with *AIPL1* deficiency.[39,75]

In a recent study evaluating the effects of cGMP accumulation on the death of cones in an all-cone

model of CNGA3 Achromatopsia, the *Cnga3*$^{-/-}$ *Nrl*$^{-/-}$ mouse, very low levels of cGMP were observed in *Nrl*$^{-/-}$ control retinas until the latest time point evaluated, P90, when they began to increase.[45] This would be consistent with a hypothesis that hyperoxia leads to increases in intracellular Ca^{2+}, which binds GCAP1, preventing it from activating retGC1 in young *Nrl*$^{-/-}$ cones. Some level of reorganization/stabilization and sufficient lowering of Ca^{2+} to allow for retGC1 activity within at least a fraction of *Nrl*$^{-/-}$ cones is likely to have occurred by P90, an age when cGMP levels began to rise.[45] On the other hand, a drastically different Ca^{2+} homeostasis would be expected to affect the sensitivity and/or the shape of the cone photoresponse. Yet that was not observed in single-cell recordings from *Nrl*$^{-/-}$ cones, which were indistinguishable from normal S cones.[42] This appears to contradict the idea of the *Nrl*$^{-/-}$ cones having Ca^{2+} constantly elevated to the point where it blocks retGC1 activation by GCAP1. One possible explanation to reconcile the contradiction between the existing observations is that the *Nrl*$^{-/-}$ cone population is highly heterogeneous, and those that have abnormally high Ca^{2+} would not be responsive in single-cell recording procedure. Another problem with the elevated Ca^{2+} as a protective factor is that the increase in free Ca^{2+} can trigger photoreceptor degeneration.[72] Hence, if hyperoxia in *Nrl*$^{-/-}$ retinas were responsible for the effects observed in our study, its effect has to be much more complex than just affecting the metal-liganded state of GCAP1.

How do the observations made in the *Nrl*$^{-/-}$ *Gucy2e*$^{-/-}$ mouse relate to the human condition and are the therapeutic outcomes achieved in this model predictive of results in a clinical trial? We do not believe that there is shared mechanism associated with the preservation of cones in *Nrl*$^{-/-}$ mice that occurs in the absence of retGC1 and the relative foveal sparing seen in LCA1 patients. There are no reports of disorganization/rosette formation or broad areas of retinal detachment in patient foveas as seen in *Nrl* $^{-/-}$ mice.[61] In fact, LCA1 patients are generally characterized as having a normal fundus and preserved retinal laminar architecture.[39] Additionally, it is not known whether patient retinas are subjected to the hyperoxia and Ca^{2+} flux that occur in *Nrl*$^{-/-}$*Gucy2e*$^{-/-}$ mice. We believe that the supernormal therapeutic outcomes in this study are dependent on the specific set of circumstances experienced in the *Nrl*$^{-/-}$ mouse retina, the possible protective effects of early/transient retGC1 depletion, and the specific timing of gene replacement intervention. We therefore do not expect that *GUCY2D* gene replacement will confer supernormal function to LCA1 patients. However, this by no means suggests that gene replacement in patients will not be successful. It is important to note that this is now the third model of retGC1 deficiency in which AAV-mediated gene replacement has resulted in long-term restoration of retinal function, visually guided behavior, and preservation of photoreceptor structure.

Notably, we have demonstrated that the combination of AAV serotype, cellular promoter, and human transgene (*GUCY2D*) likely to be used in clinical trials restored long-term retinal function to *Nrl*$^{-/-}$*Gucy2e*$^{-/-}$ mice when treatment was administered at P45. Before this study, the only demonstration of rescue using human *GUCY2D* was achieved in the GC1KO mouse only after administration of AAV8-*GUCY2D* before eye opening ($\sim$P10).[59,76] Even then, the consistency of therapeutic response (i.e., the number of mice within a treated cohort to show improvements) was low relative to that achieved with AAV vectors delivering the murine cDNA (*Gucy2e*).[76] The reason why human retGC1 is less effective in mouse than the species-specific murine homolog ($\sim$87% similar) remains unclear. Early work also showed that, despite its ability to transiently restore useful vision to a chicken model of LCA1, bovine retGC1 was incapable of rescuing the GC1KO mouse phenotype, further highlighting the species sensitivity encountered in this system.[77] It may be because of the reduced efficiency of GCAP1 and retGC1 complex formation or function. Because retGC/GCAP complexes are unstable in detergents, *in vivo* studies to evaluate how efficiently GCs bind to and function with GCAPs of different species relative to same-species combinations will be difficult. *In vitro* studies are also not necessarily predictive because of the inability to recapitulate the compartmentalization (IS/OS) and trafficking machinery of photoreceptors in a dish.[14] Nevertheless, the significant extension of the window of therapy and improvements in therapeutic outcome highlight the utility of the *Nrl*$^{-/-}$*Gucy2e*$^{-/-}$ mouse model for testing of candidate clinical vectors. LCA1 patient characterization points to the cone-rich fovea as a treatment target. Our results showing the ability to restore cone structure and function in an all-cone model of LCA1, as well as our previous finding of robust AAV5-hGRK1-mediated transgene expression in foveal/parafoveal/perifoveal cones in subretinally injected primates (macaque), have further refined our strategy for clinical application of this therapy.

ACKNOWLEDGMENTS

This study was supported by grants from the Foundation Fighting Blindness; National Institutes of Health (RO1EY024280 to S.E.B., R01EY11522 to A.M.D., R01EY019490 to X-Q.D., and P30EY021721 to W.W.H.); Creed's Cause Foundation; the Overstreet endowment; and unrestricted funding from the Research to Prevent Blindness.

We would like to acknowledge Dr. Swaroop for creation of the $Nrl^{-/-}$ mouse line. We thank Drs. Baehr, Molday, and Ramamurthy for contributing reagents. Finally, we would like to acknowledge the efforts of Dr. Samuel G. Jacobson, who continues to characterize *GUCY2D* LCA1 patients and offer guidance on the safest and most effective path toward clinical application.

AUTHOR DISCLOSURE

S.E.B., S.L.B., and W.W.H. have a U.S. patent pending (61/327,521) related to the use of AAV for the treatment of *GUCY2D*-LCA1. W.W.H. and the University of Florida have a financial interest in the use of AAV therapies and own equity in a company (AGTC, Inc.) that might, in the future, commercialize AAV vectors for the treatment of blindness. J.J.P., S.C., S.H.M., Q.R., K.T.M., Z.Z., E.V.O., I.V.O., X.Q.D., and A.M.D. have no conflicts to report.

REFERENCES

1. Burns ME, Arshavsky VY. Beyond counting photons: trials and trends in vertebrate visual transduction. Neuron 2005;48:387–401.
2. Polans A, Baehr W, Palczewski K. Turned on by Ca2+! The physiology and pathology of Ca(2+)-binding proteins in the retina. Trends Neurosci 1996;19:547–554.
3. Shyjan AW, de Sauvage FJ, Gillett NA, et al. Molecular cloning of a retina-specific membrane guanylyl cyclase. Neuron 1992;9:727–737.
4. Margulis A, Goraczniak RM, Duda T, et al. Structural and biochemical identity of retinal rod outer segment membrane guanylate cyclase. Biochem Biophys Res Commun 1993;194:855–861.
5. Dizhoor AM, Lowe DG, Olshevskaya EV, et al. The human photoreceptor membrane guanylyl cyclase, RetGC, is present in outer segments and is regulated by calcium and a soluble activator. Neuron 1994;12:1345–1352.
6. Goraczniak RM, Duda T, Sitaramayya A, et al. Structural and functional characterization of the rod outer segment membrane guanylate cyclase. Biochem J 1994;302:455–461.
7. Goraczniak R, Duda T, Sharma RK. Structural and functional characterization of a second subfamily member of the calcium-modulated bovine rod outer segment membrane guanylate cyclase, ROS-GC2. Biochem Biophys Res Commun 1997;234:666–670.
8. Palczewski K, Subbaraya I, Gorczyca WA, et al. Molecular cloning and characterization of retinal photoreceptor guanylyl cyclase-activating protein. Neuron 1994;13:395–404.
9. Lowe DG, Dizhoor AM, Liu K, et al. Cloning and expression of a second photoreceptor-specific membrane retina guanylyl cyclase (RetGC), RetGC-2. Proc Natl Acad Sci USA 1995;92:5535–5539.
10. Yang RB, Foster DC, Garbers DL, et al. Two membrane forms of guanylyl cyclase found in the eye. Proc Natl Acad Sci USA 1995;92:602–606.
11. Imanishi Y, Yang L, Sokal I, et al. Diversity of guanylate cyclase-activating proteins (GCAPs) in teleost fish: characterization of three novel GCAPs (GCAP4, GCAP5, GCAP7) from zebrafish (Danio rerio) and prediction of eight GCAPs (GCAP1-8) in pufferfish (Fugu rubripes). J Mol Evol 2004;59:204–217.
12. Imanishi Y, Li N, Sokal I, et al. Characterization of retinal guanylate cyclase-activating protein 3 (GCAP3) from zebrafish to man. Eur J Neurosci 2002;15:63–78.
13. Liu X, Seno K, Nishizawa Y, et al. Ultrastructural localization of retinal guanylate cyclase in human and monkey retinas. Exp Eye Res 1994;59:761–768.
14. Olshevskaya EV, Peshenko IV, Savchenko AB, et al. Retinal guanylyl cyclase isozyme 1 is the preferential *in vivo* target for constitutively active GCAP1 mutants causing congenital degeneration of photoreceptors. J Neurosc 2012;32:7208–7217.
15. Perrault I, Rozet JM, Calvas P, et al. Retinal-specific guanylate cyclase gene mutations in Leber's congenital amaurosis. Nat Genet 1996;14:461–464.
16. Kelsell RE, Gregory-Evans K, Payne AM, et al. Mutations in the retinal guanylate cyclase (RETGC-1) gene in dominant cone-rod dystrophy. Hum Mol Genet 1998;7:1179–1184.
17. Weigell-Weber M, Fokstuen S, Torok B, et al. Codons 837 and 838 in the retinal guanylate cyclase gene on chromosome 17p: hot spots for mutations in autosomal dominant cone-rod dystrophy? Arch Ophthalmol 2000;118:300.
18. Ugur Iseri SA, Durlu YK, Tolun A. A novel recessive GUCY2D mutation causing cone-rod dystrophy and not Leber's congenital amaurosis. Eur J Hum Genet 2010;18:1121–1126.
19. Jiang L, Katz BJ, Yang Z, et al. Autosomal dominant cone dystrophy caused by a novel mutation in the GCAP1 gene (GUCA1A). Mol Vis 2005;11:143–151.
20. Nishiguchi KM, Sokal I, Yang L, et al. A novel mutation (I143NT) in guanylate cyclase-activating protein 1 (GCAP1) associated with autosomal dominant cone degeneration. Invest Ophthalmol Vis Sci 2004;45:3863–3870.
21. Sokal I, Dupps WJ, Grassi MA, et al. A novel GCAP1 missense mutation (L151F) in a large family with autosomal dominant cone-rod dystrophy (adCORD). Invest Ophthalmol Vis Sci 2005;46:1124–1132.
22. Payne AM, Downes SM, Bessant DA, et al. A mutation in guanylate cyclase activator 1A (GUCA1A) in an autosomal dominant cone dystrophy pedigree mapping to a new locus on chromosome 6p21.1. Hum Mol Genet 1998;7:273–277.
23. Downes SM, Holder GE, Fitzke FW, et al. Autosomal dominant cone and cone-rod dystrophy with mutations in the guanylate cyclase activator 1A gene-encoding guanylate cyclase activating protein-1. Arch Ophthalmol 2001;119:96–105.
24. Wilkie SE, Li Y, Deery EC, et al. Identification and functional consequences of a new mutation (E155G) in the gene for GCAP1 that causes autosomal dominant cone dystrophy. Am J Hum Genet 2001;69:471–480.
25. Michaelides M, Wilkie SE, Jenkins S, et al. Mutation in the gene GUCA1A, encoding guanylate cyclase-activating protein 1, causes cone, cone-rod, and macular dystrophy. Ophthalmology 2005;112:1442–1447.
26. Kitiratschky VB, Behnen P, Kellner U, et al. Mutations in the GUCA1A gene involved in hereditary cone dystrophies impair calcium-mediated regulation of guanylate cyclase. Hum Mutat 2009;30:E782–E796.

27. Boye SE, Boye SL, Lewin AS, et al. A comprehensive review of retinal gene therapy. Mol Ther 2013;21:509–519.
28. Maguire AM, Simonelli F, Pierce EA, et al. Safety and efficacy of gene transfer for Leber's congenital amaurosis. N Engl J Med 2008;358: 2240–2248.
29. Bainbridge JW, Smith AJ, Barker SS, et al. Effect of gene therapy on visual function in Leber's congenital amaurosis. N Engl J Med 2008;358: 2231–2239.
30. Cideciyan AV, Aleman TS, Boye SL, et al. Human gene therapy for RPE65 isomerase deficiency activates the retinoid cycle of vision but with slow rod kinetics. Proc Natl Acad Sci USA 2008;105: 15112–15117.
31. MacLaren RE, Groppe M, Barnard AR, et al. Retinal gene therapy in patients with choroideremia: initial findings from a phase 1/2 clinical trial. Lancet 2014;383:1129-1137.
32. Boye SE, Boye SL, Pang J, et al. Functional and behavioral restoration of vision by gene therapy in the guanylate cyclase-1 (GC1) knockout mouse. PLoS One 2010;5:e11306.
33. Boye SL, Conlon T, Erger K, et al. Long-term preservation of cone photoreceptors and restoration of cone function by gene therapy in the guanylate cyclase-1 knockout (GC1KO) mouse. Invest Ophthalmol Vis Sci 2011;52:7098–7108.
34. Boye SL, Peshenko IV, Huang WC, et al. AAV-mediated gene therapy in the guanylate cyclase (RetGC1/RetGC2) double knockout mouse model of Leber congenital amaurosis. Hum Gene Ther 2013;24:189–202.
35. Yang RB, Robinson SW, Xiong WH, et al. Disruption of a retinal guanylyl cyclase gene leads to cone-specific dystrophy and paradoxical rod behavior. J Neurosci 1999;19:5889–5897.
36. Baehr W, Karan S, Maeda T, et al. The function of guanylate cyclase 1 (GC1) and guanylate cyclase 2 (GC2) in rod and cone photoreceptors. J Biol Chem 2007;282:8837–8847.
37. Milam AH, Barakat MR, Gupta N, et al. Clinicopathologic effects of mutant GUCY2D in Leber congenital amaurosis. Ophthalmology 2003;110: 549–558.
38. Porto FB, Perrault I, Hicks D, et al. Prenatal human ocular degeneration occurs in Leber's Congenital Amaurosis (LCA1 and 2). Adv Exp Med Biol 2003;533:59–68.
39. Jacobson SG, Cideciyan AV, Peshenko IV, et al. Determining consequences of retinal membrane guanylyl cyclase (RetGC1) deficiency in human Leber congenital amaurosis en route to therapy: residual cone-photoreceptor vision correlates with biochemical properties of the mutants. Hum Mol Genet 2013;22:168–183.
40. Peichl L. Diversity of mammalian photoreceptor properties: adaptations to habitat and lifestyle? Anat Rec A Discov Mol Cell Evol Biol 2005;287: 1001–1012.
41. Blanks JC, Johnson LV. Specific binding of peanut lectin to a class of retinal photoreceptor cells. A species comparison. Invest Ophthalmol Vis Sci 1984;25:546–557.
42. Daniele LL, Lillo C, Lyubarsky AL, et al. Cone-like morphological, molecular, and electrophysiological features of the photoreceptors of the Nrl knockout mouse. Invest Ophthalmol Vis Sci 2005; 46:2156–2167.
43. Mears AJ, Kondo M, Swain PK, et al. Nrl is required for rod photoreceptor development. Nat Genet 2001;29:447–452.
44. Nikonov SS, Daniele LL, Zhu X, et al. Photoreceptors of $Nrl^{-/-}$ mice coexpress functional S- and M-cone opsins having distinct inactivation mechanisms. J Gen Physiol 2005;125:287–304.
45. Xu J, Morris L, Thapa A, et al. cGMP accumulation causes photoreceptor degeneration in CNG channel deficiency: evidence of cGMP cytotoxicity independently of enhanced CNG channel function. J Neurosci 2013;33:14939–14948.
46. Kolandaivelu S, Singh RK, Ramamurthy V. AIPL1, a protein linked to blindness, is essential for the stability of enzymes mediating cGMP metabolism in cone photoreceptor cells. Hum Mol Genet 2014;23:1002–1012.
47. Boye SE, Huang WC, Roman AJ, et al. Natural history of cone disease in the murine model of Leber congenital amaurosis due to CEP290 mutation: determining the timing and expectation of therapy. PloS One 2014;9:e92928.
48. Khani SC, Pawlyk BS, Bulgakov OV, et al. AAV-mediated expression targeting of rod and cone photoreceptors with a human rhodopsin kinase promoter. Invest Ophthalmol Vis Sci 2007;48: 3954-3961.
49. Zolotukhin S, Potter M, Zolotukhin I, et al. Production and purification of serotype 1, 2, and 5 recombinant adeno-associated viral vectors. Methods 2002;28:158–167.
50. Jacobson SG, Acland GM, Aguirre GD, et al. Safety of recombinant adeno-associated virus type 2-RPE65 vector delivered by ocular subretinal injection. Mol Ther 2006;13:1074–1084.
51. Timmers AM, Zhang H, Squitieri A, et al. Subretinal injections in rodent eyes: effects on electrophysiology and histology of rat retina. Mol Vis 2001;7:131–137.
52. Boye SE, Alexander JJ, Boye SL, et al. The human rhodopsin kinase promoter in an AAV5 vector confers rod- and cone-specific expression in the primate retina. Hum Gene Ther 2012;23:1101–1115.
53. Cideciyan AV, Rachel RA, Aleman TS, et al. Cone photoreceptors are the main targets for gene therapy of NPHP5 (IQCB1) or NPHP6 (CEP290) blindness: generation of an all-cone Nphp6 hypomorph mouse that mimics the human retinal ciliopathy. Hum Mol Genet 2011;20:1411–1423.
54. Prusky GT, Alam NM, Beekman S, et al. Rapid quantification of adult and developing mouse spatial vision using a virtual optomotor system. Invest Ophthalmol Vis Sci 2004;45:4611–4616.
55. Olshevskaya EV, Calvert PD, Woodruff ML, et al. The Y99C mutation in guanylyl cyclase-activating protein 1 increases intracellular Ca2+ and causes photoreceptor degeneration in transgenic mice. J Neurosci 2004;24:6078–6085.
56. Peshenko IV, Olshevskaya EV, Savchenko AB, et al. Enzymatic properties and regulation of the native isozymes of retinal membrane guanylyl cyclase (RetGC) from mouse photoreceptors. Biochemistry 2011;50:5590–5600.
57. Pang JJ, Dai X, Boye SE, et al. Long-term retinal function and structure rescue using capsid mutant AAV8 vector in the rd10 mouse, a model of recessive retinitis pigmentosa. Mol Ther 2011;19:234–242.
58. Haire SE, Pang J, Boye SL, et al. Light-driven cone arrestin translocation in cones of postnatal guanylate cyclase-1 knockout mouse retina treated with AAV-GC1. Invest Ophthalmol Vis Sci 2006;47: 3745–3753.
59. Mihelec M, Pearson RA, Robbie SJ, et al. Long-term preservation of cones and improvement in visual function following gene therapy in a mouse model of leber congenital amaurosis caused by guanylate cyclase-1 deficiency. Hum Gene Ther 2011;22:1179–1190.
60. Coleman JE, Zhang Y, Brown GA, et al. Cone cell survival and downregulation of GCAP1 protein in the retinas of GC1 knockout mice. Invest Ophthalmol Vis Sci 2004;45:3397–3403.
61. Roger JE, Ranganath K, Zhao L, et al. Preservation of cone photoreceptors after a rapid yet transient degeneration and remodeling in cone-only $Nrl^{-/-}$ mouse retina. J Neurosci 2012;32:528–541.
62. Semple-Rowland SL, Gorczyca WA, Buczylko J, et al. Expression of GCAP1 and GCAP2 in the retinal degeneration (rd) mutant chicken retina. FEBS Lett 1996;385:47–52.
63. Azadi S, Molday LL, Molday RS. RD3, the protein associated with Leber congenital amaurosis type 12, is required for guanylate cyclase trafficking in photoreceptor cells. Proc Natl Acad Sci USA 2010;107:21158–21163.
64. Zulliger R, Naash MI, Rajala RV, et al. Impaired association of retinal degeneration-3 with guanylate cyclase-1 and guanylate cyclase activating protein-1 leads to Leber congenital amaurosis-1. J Biol Chem 2015;290:3488–3499.
65. Molday LL, Djajadi H, Yan P, et al. RD3 gene delivery restores guanylate cyclase localization and rescues photoreceptors in the Rd3 mouse model of Leber congenital amaurosis 12. Hum Mol Genet 2013;22:3894–3905.
66. Karan S, Frederick JM, Baehr W. Novel functions of photoreceptor guanylate cyclases revealed by targeted deletion. Mol Cell Biochem 2010;334: 141–155.
67. Mancuso K, Hauswirth WW, Li Q, et al. Gene therapy for red-green colour blindness in adult primates. Nature 2009;461:784–787.

68. Sanvicens N, Gomez-Vicente V, Masip I, et al. Oxidative stress-induced apoptosis in retinal photoreceptor cells is mediated by calpains and caspases and blocked by the oxygen radical scavenger CR-6. J Biol Chem 2004;279:39268–39278.

69. Berridge MJ, Bootman MD, Lipp P. Calcium—a life and death signal. Nature 1998;395:645–648.

70. He L, Poblenz AT, Medrano CJ, et al. Lead and calcium produce rod photoreceptor cell apoptosis by opening the mitochondrial permeability transition pore. J Biol Chem 2000;275:12175–12184.

71. Dizhoor AM, Boikov SG, Olshevskaya EV. Constitutive activation of photoreceptor guanylate cyclase by Y99C mutant of GCAP-1. Possible role in causing human autosomal dominant cone degeneration. J Biol Chem 1998;273:17311–17314.

72. Dell'Orco D, Behnen P, Linse S, et al. Calcium binding, structural stability and guanylate cyclase activation in GCAP1 variants associated with human cone dystrophy. Cell Mol Life Sci 2010;67:973–984.

73. Lim S, Peshenko I, Dizhoor A, et al. Effects of Ca2+, Mg2+, and myristoylation on guanylyl cyclase activating protein 1 structure and stability. Biochemistry 2009;48:850–862.

74. Tosi J, Davis RJ, Wang NK, et al. shRNA knockdown of guanylate cyclase 2e or cyclic nucleotide gated channel alpha 1 increases photoreceptor survival in a cGMP phosphodiesterase mouse model of retinitis pigmentosa. J Cell Mol Med 2011;15:1778–1787.

75. Jacobson SG, Cideciyan AV, Aleman TS, et al. Human retinal disease from AIPL1 gene mutations: foveal cone loss with minimal macular photoreceptors and rod function remaining. Invest Ophthalmol Vis Sci 2011;52:70–79.

76. Manfredi A, Marrocco E, Puppo A, et al. Combined rod and cone transduction by adeno-associated virus 2/8. Hum Gene Ther 2013;24:982–992.

77. Williams ML, Coleman JE, Haire SE, et al. Lentiviral expression of retinal guanylate cyclase-1 (RetGC1) restores vision in an avian model of childhood blindness. PLoS Med 2006;3:e201.

Received for publication April 28, 2015;
accepted after revision May 29, 2015.

Published online: June 2, 2015.